



## Research Article

<https://doi.org/10.1631/jzus.B2300154>

# *RAD51B-AS1* promotes the malignant biological behavior of ovarian cancer through upregulation of *RAD51B*

Xinyi WEI<sup>1</sup>, Conghui WANG<sup>2</sup>, Sangsang TANG<sup>2</sup>, Qian YANG<sup>2</sup>, Zhangjin SHEN<sup>1</sup>, Jiawei ZHU<sup>2</sup>, Xiaodong CHENG<sup>2</sup>, Xinyu WANG<sup>2,4</sup>, Xing XIE<sup>2†</sup>, Junfen XU<sup>2,5✉</sup>, Weiguo LU<sup>2,3,5✉</sup>

<sup>1</sup>Women's Reproductive Health Laboratory of Zhejiang Province, Women's Hospital, Zhejiang University School of Medicine, Hangzhou 310006, China

<sup>2</sup>Department of Gynecologic Oncology, Women's Hospital, Zhejiang University School of Medicine, Hangzhou 310006, China

<sup>3</sup>Cancer Center, Zhejiang University, Hangzhou 310058, China

<sup>4</sup>Department of Obstetrics and Gynecology, the First Affiliated Hospital, Zhejiang University School of Medicine, Hangzhou 310003, China

<sup>5</sup>Zhejiang Provincial Clinical Research Center for Obstetrics and Gynecology, Hangzhou 310006, China

**Abstract:** Long non-coding RNAs (lncRNAs) play an indispensable role in the occurrence and development of ovarian cancer (OC). However, the potential involvement of lncRNAs in the progression of OC is largely unknown. To investigate the detailed roles and mechanisms of RAD51 homolog B-antisense 1 (*RAD51B-AS1*), a novel lncRNA in OC, reverse transcription-quantitative polymerase chain reaction (RT-qPCR) was performed to verify the expression of *RAD51B-AS1*. Cellular proliferation, metastasis, and apoptosis were detected using the cell counting kit-8 (CCK-8), colony-formation, transwell, and flow cytometry assays. Mouse xenograft models were established for the detection of tumorigenesis. The results revealed that *RAD51B-AS1* was significantly upregulated in a highly metastatic human OC cell line and OC tissues. *RAD51B-AS1* significantly increased the proliferation and metastasis of OC cells and enhanced their resistance to anoikis. Biogenetics prediction analysis revealed that the only target gene of *RAD51B-AS1* was *RAD51B*. Subsequent gene function experiments revealed that *RAD51B* exerts the same biological effects as *RAD51B-AS1*. Rescue experiments demonstrated that the malignant biological behaviors promoted by *RAD51B-AS1* overexpression were partially or completely reversed by *RAD51B* silencing in vitro and in vivo. Thus, *RAD51B-AS1* promotes the malignant biological behaviors of OC and activates the protein kinase B (Akt)/B cell lymphoma protein-2 (Bcl-2) signaling pathway, and these effects may be associated with the positive regulation of *RAD51B* expression. *RAD51B-AS1* is expected to serve as a novel molecular biomarker for the diagnosis and prediction of poor prognosis in OC, and as a potential therapeutic target for disease management.

**Key words:** Ovarian cancer (OC); Long non-coding RNA (lncRNA); Metastasis; Anoikis

## 1 Introduction

Ovarian cancer (OC) has the highest fatality rate among all gynecologic malignancies (Torre et al., 2018; Sung et al., 2021). Due to the deep location of the ovary within the pelvic cavity, inconspicuous early symptoms, and lack of specific tumor markers, >75%

of patients with OC are initially diagnosed with late-stage disease (International Federation of Gynecology and Obstetrics (FIGO) stages III and IV), as well as abdominal cavity metastasis and/or distant metastases (US Preventive Services Task Force, 2018; Lheureux et al., 2019; Xie et al., 2021). Therefore, a thorough understanding of the molecular mechanisms underlying the development of OC, along with the elucidation of interventional measures, is urgently required.

Long non-coding RNAs (lncRNAs) consist of >200 nucleotides (nt) with limited or no protein-coding function (Bhan et al., 2017). A growing number of lncRNAs have been reported to participate in the procession of OC through a variety of pathways and

<sup>†</sup> Xing XIE is deceased

✉ Junfen XU, [xjfu@zju.edu.cn](mailto:xjfu@zju.edu.cn)

Weiguo LU, [lbwg@zju.edu.cn](mailto:lbwg@zju.edu.cn)

✉ Xinyi WEI, <https://orcid.org/0009-0008-5637-1704>

Junfen XU, <https://orcid.org/0000-0002-2377-0775>

Weiguo LU, <https://orcid.org/0000-0003-2062-7145>

Received Mar. 9, 2023; Revision accepted Aug. 29, 2023;  
Crosschecked June 3, 2024

© Author(s) 2024

molecular mechanisms (Wu et al., 2017, 2021; Liang et al., 2018; Pei et al., 2020; Yang et al., 2021; Zhao et al., 2021). However, no efficient and specific lncRNA has been identified or used for OC diagnosis or treatment, and the clinical significance and biological mechanisms of the overwhelming majority of lncRNAs remain unknown, highlighting the need to identify novel lncRNAs as potential molecular markers for OC.

Here, we identified a novel and previously uncharacterized lncRNA, ENST00000554679.1 (*RAD51* homolog B-antisense 1 (*RAD51B-AS1*)), located on 14q24.1. It consists of two exons and is transcribed from the reverse strand of the *RAD51B* gene. We hypothesize that *RAD51B-AS1* acts as an oncogene in OC by upregulating *RAD51B*. This study investigated the expression, role, and potential mechanism of *RAD51B-AS1* in OC development. The results of this study may facilitate the elucidation of potential diagnostic or therapeutic OC biomarkers. *RAD51B-AS1* may serve as a predictor of poor prognosis in OC and as a potential therapeutic target for disease management.

## 2 Results

### 2.1 Identification and characterization of *RAD51B-AS1*

The lncRNA expression profiles of the ovarian carcinoma cell line HO8910 and the derived cell line HO8910PM, which has a higher malignancy than HO8910 (Shen XM et al., 2021; Shen ZJ et al., 2022), were analyzed using high-throughput sequencing analysis (Fig. 1a). The top 16 differentially expressed lncRNAs ( $\log_2(\text{fold change}) > 2.5$  or  $< -2.5$ ,  $P < 0.05$ ) were selected for further validation (Tables S1 and S2). Among the selected lncRNAs, *RAD51B-AS1* was determined to be the most significantly upregulated following reverse transcription-quantitative polymerase chain reaction (RT-qPCR) (Fig. 1b). *RAD51B-AS1* was 537 nt in length and was confirmed in the present study using northern blotting (Fig. 1c). It was predominantly located in the nucleus, as verified by subcellular fractionation, expression analysis (Fig. 1d), and fluorescence in situ hybridization (FISH) analysis (Fig. 1e). The current study assessed *RAD51B-AS1* expression in 49 ovarian carcinoma tissues and eight nonmalignant ovaries, revealing a remarkable increase in the expression of *RAD51B-AS1* in cancer samples (Fig. 1f).

### 2.2 Effects of lncRNA *RAD51B-AS1* on growth, metastasis, and anoikis resistance in OC cells

Knockdown and overexpression experiments were performed to clarify the biological functional roles of *RAD51B-AS1* in malignant OC cells. *RAD51B-AS1* was knocked down using two small interfering RNAs (siRNAs) transfected into HO8910PM cells, which were selected because of their relatively higher expression of *RAD51B-AS1*. Knockdown experiments demonstrated a high knockdown efficiency (Fig. 2a). In addition, a *RAD51B-AS1* overexpression lentivirus was transduced into HO8910 ovarian cells, which possess lower level of *RAD51B-AS1*, to establish a cell line that was stably overexpressing *RAD51B-AS1*. The efficiency of this experiment was also demonstrated (Fig. 2b). Cell counting kit-8 (CCK-8) assays revealed that the proliferation of cells was significantly attenuated after the depletion of endogenous *RAD51B-AS1* (Fig. 2c) and increased considerably after *RAD51B-AS1* overexpression (Fig. 2d). Similar trends were observed in colony-formation and survival assays following *RAD51B-AS1* knockdown (Fig. 2e) and overexpression (Fig. 2f). The migration and invasion of cells were markedly lower in the *RAD51B-AS1* knockdown group than in the control group (Fig. 2g), while the *RAD51B-AS1* overexpression group significantly increased the migration and invasion of cells (Fig. 2h). We found that the highly metastatic cell line HO8910PM demonstrated stronger anoikis resistance than the parent cell line HO8910 (Fig. S1a), indicating that this may be the mechanism underlying stronger metastasis. To investigate this hypothesis, functional assays of the anoikis resistance conferred by *RAD51B-AS1* were performed. The results revealed that *RAD51B-AS1* knockdown significantly increased the apoptotic rate of anoikis-resistant cells (Fig. 2i), whereas overexpression of *RAD51B-AS1* significantly reduced these effects (Fig. 2j). In the soft-agar assay, the anchor-independent growth of OC cells was significantly weakened after *RAD51B-AS1* silencing (Fig. S1b) and was enhanced after *RAD51B-AS1* overexpression (Fig. S1c). Since B cell lymphoma protein-2 (*Bcl-2*) is an anti-anoikis gene, its protein expression levels were reduced following *RAD51B-AS1* downregulation (Fig. 2k) and increased with *RAD51B-AS1* overexpression (Fig. 2l). Furthermore, the intracellular RNA levels of lncRNA *RAD51B-AS1* were significantly increased after induction of the suspension for 24 and 48 h (Fig. 2m).

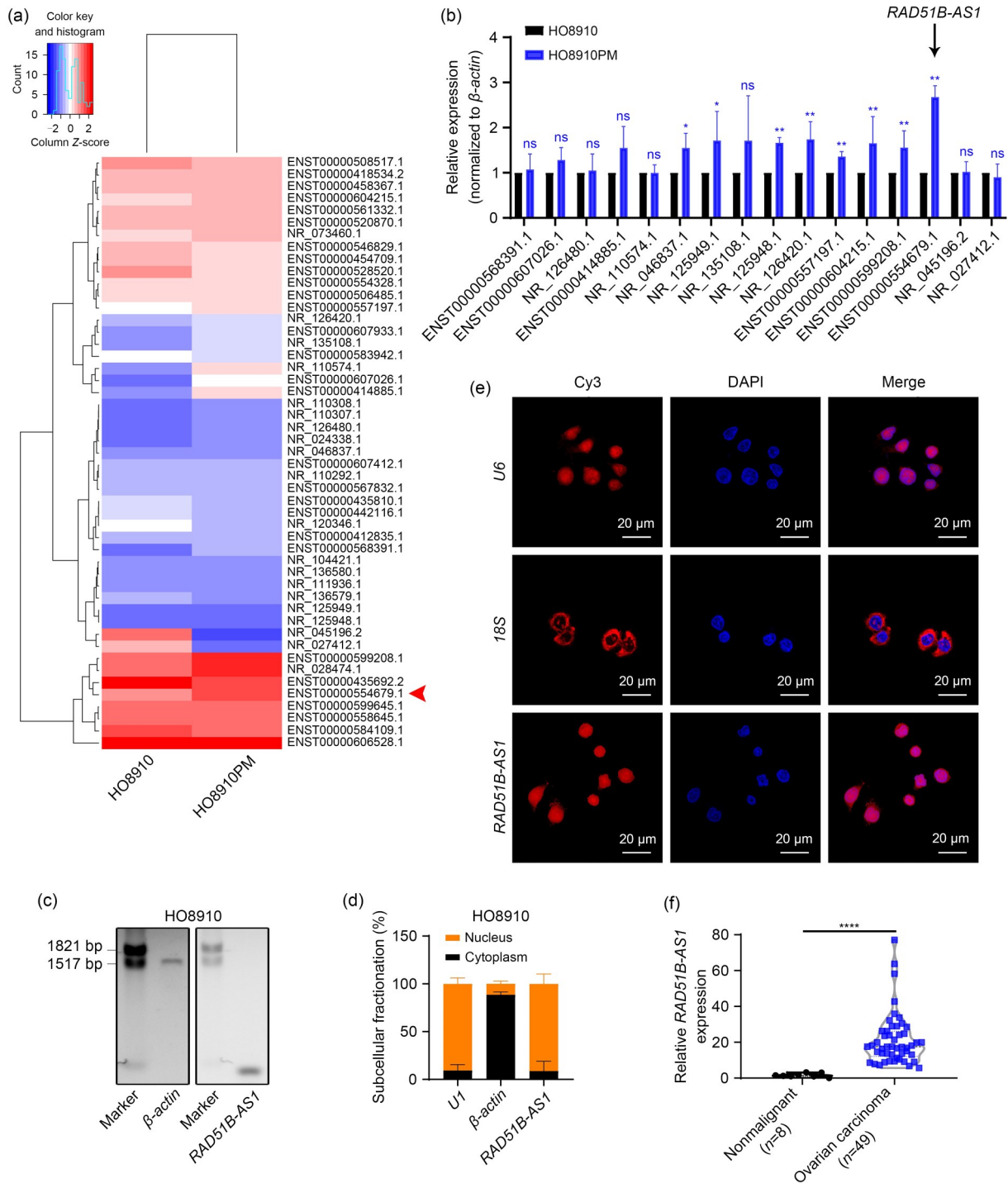


**Fig. 1** Identification and characterization of *RAD51B-AS1*. (a) Heatmap of differentially expressed lncRNAs between HO8910 ( $n=1$ ) and HO8910PM ( $n=1$ ) ( $\log_2$ (fold change) $>2$  or  $<-2$ ,  $P < 0.05$ ). The red arrowhead indicates lncRNA *RAD51B-AS1*. (b) The expression levels of 16 selected lncRNAs were detected by RT-qPCR in HO8910 and HO8910PM cells. Results are shown as mean $\pm$ SD ( $n \geq 3$ ). \*  $P < 0.05$ , \*\*  $P < 0.01$ , vs. HO8910. (c) The validation of *RAD51B-AS1* using northern blotting. (d) Subcellular fractionation detection showed the location of *RAD51B-AS1*. Results are shown as mean $\pm$ SD ( $n=3$ ). (e) FISH assay showed the location of *RAD51B-AS1* with U6 and 18S as internal references. (f) The expression of *RAD51B-AS1* in nonmalignant ovarian tissues and ovarian cancer (OC) tissues. \*\*\*\*  $P < 0.0001$ . *RAD51B-AS1*: RAD51 homolog B-antisense 1; LncRNAs: long non-coding RNAs; RT-qPCR: reverse transcription-quantitative polymerase chain reaction; SD: standard deviation; ns: not significant; FISH: fluorescence in situ hybridization; Cy3: cyanine 3; DAPI: 4',6-diamidino-2-phenylindole.

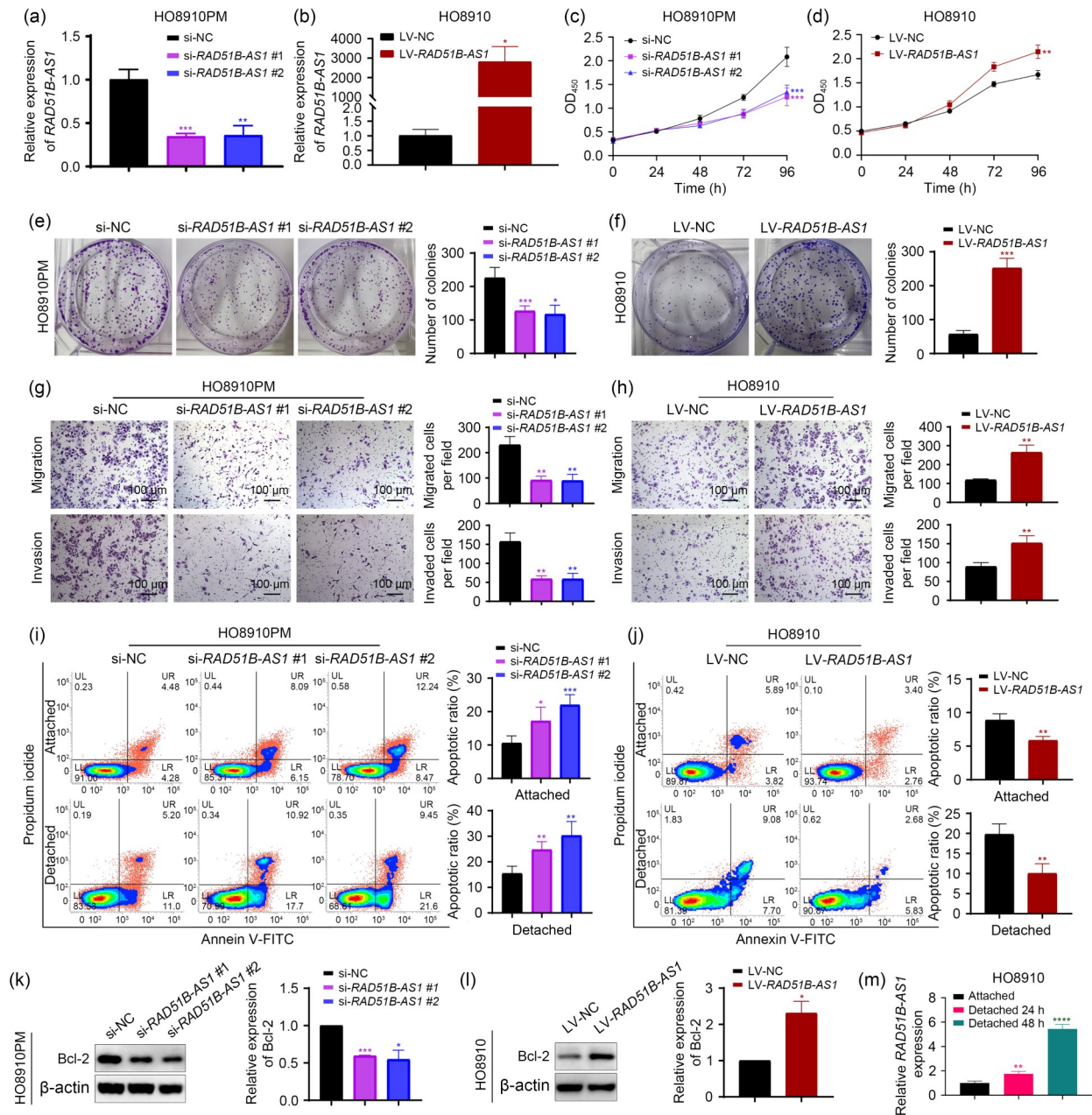


**Fig. 2** Effects of lncRNA *RAD51B-AS1* on growth, metastasis, and anoikis resistance in ovarian cancer cells. (a) Verification of the knockdown efficiency of two specific siRNAs targeting *RAD51B-AS1* in HO8910PM cells using RT-qPCR analysis. (b) Verification of the efficiency of lentivirus overexpression in HO8910 cells using RT-qPCR analysis. (c, d) CCK-8 assays showed proliferation of HO8910 and HO8910PM cells after knockdown (c) or overexpression (d) of *RAD51B-AS1*. (e, f) Representative images of colony-formation assays for the survival ability in HO8910PM and HO8910 cells after *RAD51B-AS1* downregulation (e) and upregulation (f) are shown in the left panels. Statistics for colony numbers per well are shown in the right graphs. (g, h) Transwell assays demonstrated the migration and invasion ability after knockdown (g) or overexpression (h) of *RAD51B-AS1*. (i, j) Flow cytometry analyses of apoptosis rates after knockdown (i) or overexpression (j) of *RAD51B-AS1*. (k, l) Western blotting assays showed expression of Bcl-2 protein after dysregulation of *RAD51B-AS1*. (m) The expression level of *RAD51B-AS1* was detected by RT-qPCR in HO8910 cells at 24 and 48 h after induction of the suspension. Results are shown as mean $\pm$ SD,  $n \geq 3$ . \*  $P < 0.05$ , \*\*  $P < 0.01$ , \*\*\*  $P < 0.001$ , \*\*\*\*  $P < 0.0001$ , vs. the control group or the attached group. LncRNA: long non-coding RNA; *RAD51B-AS1*: RAD51 homolog B-antisense 1; si: small interfering; RT-qPCR: reverse transcription-quantitative polymerase chain reaction; CCK-8: cell counting kit-8; Bcl-2: B cell lymphoma protein-2; SD: standard deviation; OD<sub>450</sub>: optical density at 450 nm; NC: negative control; LV: lentivirus; FITC: fluorescein isothiocyanate.

compared with adherent HO8910 cells, indicating that *RAD51B-AS1* contributed to anoikis resistance in OC.

### 2.3 Regulation of *RAD51B* by *RAD51B-AS1*

A biogenetic prediction analysis of the downstream target genes of *RAD51B-AS1* was conducted. Since *RAD51B-AS1* is mainly located in the nucleus, the mechanisms by which it regulates its target genes can be primarily divided into cis- and trans-regulation. Potential target genes of cis-regulated lncRNAs were identified by integrating the differentially expressed lncRNAs with their adjacent (10 kb) messenger RNA (mRNA) data. For the prediction of trans-regulation, sequences of differentially expressed lncRNAs and mRNAs were first extracted, after which BLAST software (US National Library of Medicine, USA) was used for primary screening and RNAPlex software (Tafer and Hofacker, 2008) was used for secondary screening to identify the possible target genes of lncRNAs. As demonstrated in Tables S3 and S4, the only target gene identified was *RAD51B*.

FISH assays revealed that *RAD51B-AS1* and *RAD51B* were both located in the nucleus in close proximity to each other; with stable overexpression of *RAD51B-AS1*, the fluorescence intensity of *RAD51B* also increased (Fig. 3a). Data from 49 OC cases were subsequently analyzed, and the findings showed clear evidence of a positive linear correlation between *RAD51B-AS1* and *RAD51B* (Fig. 3b). To verify whether *RAD51B* is the target gene of *RAD51B-AS1*, RT-qPCR and western blotting assays were performed. Owing to the position of *RAD51B-AS1* corresponding to the intron of *RAD51B*, the two transfected siRNAs did not have any effect on *RAD51B* mRNA levels (Fig. S2a). *RAD51B-AS1* knockdown and overexpression markedly decreased and increased *RAD51B* mRNA expression levels, respectively (Figs. 3c and 3d). Additionally, western blotting analyses revealed that *RAD51B* protein levels were markedly different (Figs. 3e and 3f), which was consistent with the mRNA levels in dysregulated *RAD51B-AS1* cell lines. These results suggest that *RAD51B-AS1* may regulate *RAD51B* expression at the transcriptional and translational levels. We hypothesized that *RAD51B-AS1* may facilitate OC progression by increasing *RAD51B* expression.

### 2.4 Promotion of the malignant biological behavior in OC by *RAD51B*

*RAD51B* expression was markedly upregulated in OC tissues (Fig. 4a) and survival plots revealed that

patients with higher *RAD51B* expression levels had lower progression-free survival (PFS) and overall survival (OS) (Fig. S2b). To determine the potential regulatory role of *RAD51B* in the malignant behavior of OC, *RAD51B* expression was downregulated in HO8910PM cells by transfection with si-*RAD51B*, which simultaneously reduced the expression of the anti-apoptotic protein Bcl-2 (Fig. 4b). Subsequently, CCK-8 (Fig. 4c) and colony-formation (Fig. 4d) assays were performed to determine the effects of *RAD51B* on OC cell proliferation. *RAD51B* silencing inhibited cell proliferation and survival. Consistent with the findings obtained for *RAD51B-AS1*, *RAD51B* downregulation also reduced metastasis (Fig. 4e) and anoikis resistance (Fig. 4f) in the HO8910PM cells. In the soft-agar assay, the anchor-independent growth of OC cells was significantly reduced after *RAD51B* knockdown (Fig. S2c). *RAD51B* was positively associated with *RAD51B-AS1* and exhibited pro-carcinogenic properties in OC.

### 2.5 Effects of *RAD51B-AS1* on OC progression and Akt/Bcl-2 pathway by regulating *RAD51B* expression

To further demonstrate that *RAD51B-AS1* may promote cancer cell progression by interfering with *RAD51B* expression, rescue assays were conducted. These assays showed that *RAD51B-AS1* overexpression markedly increased OC cell growth (Figs. 5a and S3a) and metastasis (Fig. 5b), which was abolished by *RAD51B* deletion in HO8910 cells. Similarly, *RAD51B* knockdown reversed the promotion of anoikis resistance and anchor-independent growth following *RAD51B-AS1* upregulation (Figs. 5c and S3b). Furthermore, another cell line, A2780, was selected to supplement the validation. Knockdown of *RAD51B* significantly revised enhanced cell viability (Figs. 5d and S3c), metastasis (Fig. 5e), and anoikis resistance (Figs. 5f and S3d) induced by *RAD51B-AS1* overexpression in A2780 cells. In addition, western blotting assays suggested that the expression of protein kinase B (Akt) did not change after *RAD51B-AS1* overexpression or si-*RAD51B* transfection. However, compared to control groups, phosphorylated Akt (p-Akt) and Bcl-2 expression was upregulated following LV-*RAD51B-AS1* overexpression and the enhanced effects on p-Akt and Bcl-2 expression could be partially downregulated by si-*RAD51B* in both HO8910 (Fig. 5g) and A2780 (Fig. 5h) cells. On the basis of these results, *RAD51B-AS1* mediates the activation of the Akt/Bcl-2 signaling pathway through the regulation of *RAD51B* expression.

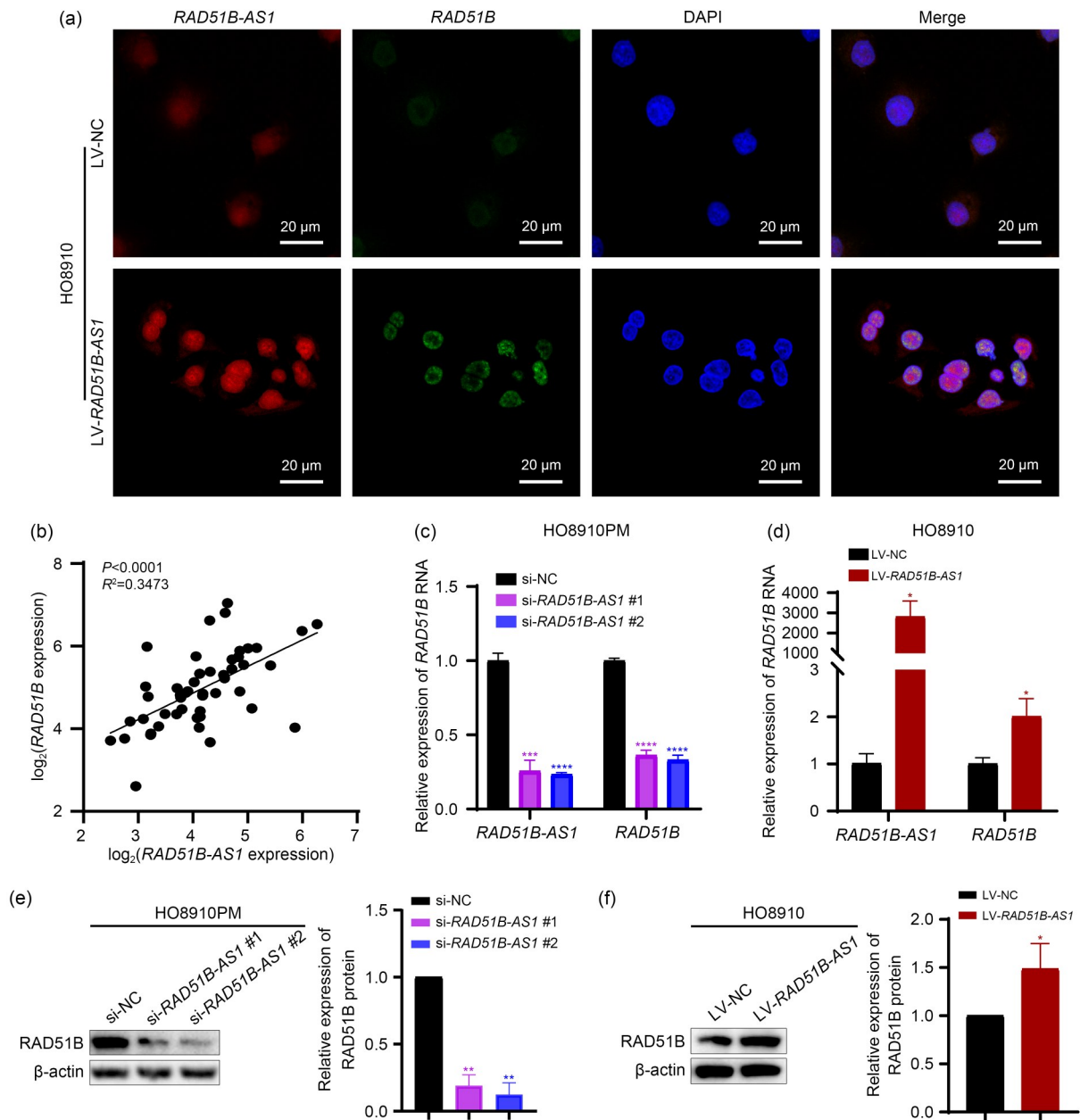


**Fig. 3** Regulation of *RAD51B* by *RAD51B-AS1*. (a) FISH and immunofluorescence co-localization showed that *RAD51B-AS1* and *RAD51B* were co-localized in the nucleus. (b) The linear correlation between *RAD51B-AS1* and *RAD51B* in 49 cases of ovarian cancer (OC) using RT-qPCR analysis. (c, d) RT-qPCR showed the mRNA levels of *RAD51B* after silencing (c) or overexpression (d) of *RAD51B-AS1*. (e, f) Western blotting analyses showed the protein level of *RAD51B* after knockdown (e) or overexpression (f) of *RAD51B-AS1*. Results are shown as mean $\pm$ SD,  $n=3$ . \*  $P < 0.05$ , \*\*  $P < 0.01$ , \*\*\*  $P < 0.001$ , \*\*\*\*  $P < 0.0001$ , vs. the control group. FISH: fluorescence in situ hybridization; RT-qPCR: reverse transcription-quantitative polymerase chain reaction; mRNA: messenger RNA; SD: standard deviation; si: small interfering; NC: negative control; LV: lentivirus; DAPI: 4',6-diamidino-2-phenylindole; *RAD51B-AS1*: RAD51 homolog B-antisense 1.

### 2.6 Effect of *RAD51B-AS1* on OC progression by regulating *RAD51B* expression in vivo

To confirm whether *RAD51B-AS1* affects OC cell proliferation through *RAD51B* in vivo, subcutaneous

tumor mouse models were established. The results revealed that, after an intratumoral injection of si-*RAD51B*, the tumor-promoting ability of the over-expressed group was significantly lower than that of the control group (Figs. 6a–6c). Both the knockdown

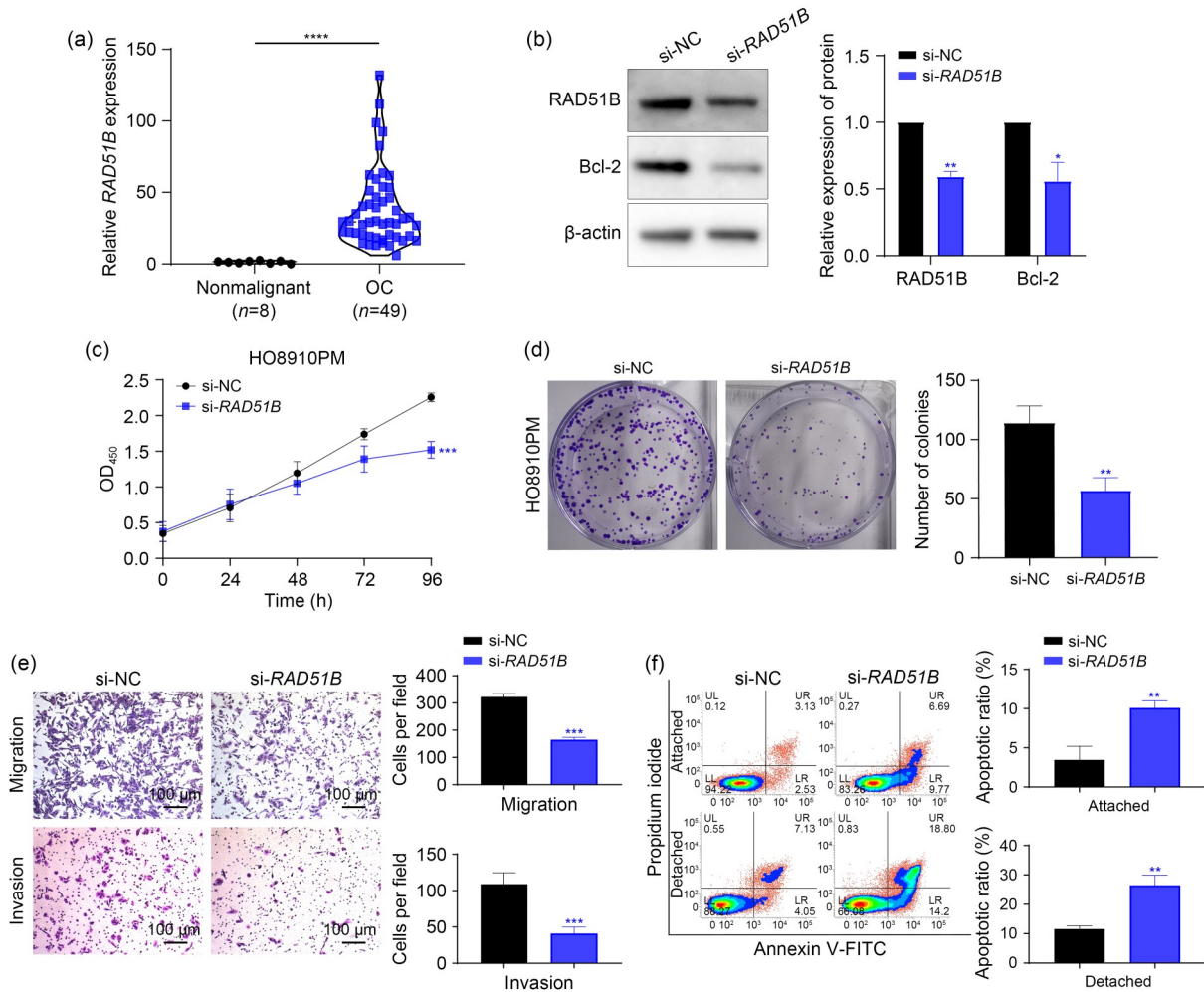


**Fig. 4** Promotion of the malignant biological behavior in ovarian cancer (OC) by *RAD51B*. (a) Comparison of *RAD51B* expression in nonmalignant ovarian tissues and OC tissues using RT-qPCR. (b) Western blotting analysis showed the expression of Bcl-2 and *RAD51B*. (c) CCK-8 assays showed cell growth ability after *RAD51B* knockdown. (d) Colony-formation assays showed the colony formation ability of HO8910PM cells. (e) Transwell assays showed cell migration and invasion after *RAD51B* knockdown. (f) Apoptosis rate after *RAD51B* knockdown. Results are shown as mean±SD,  $n=3$ . \*  $P<0.05$ , \*\*  $P<0.01$ , \*\*\*  $P<0.001$ , \*\*\*\*  $P<0.0001$ , vs. the control group. *RAD51B-ASI*: *RAD51B* homolog B-antisense 1; RT-qPCR: reverse transcription-quantitative polymerase chain reaction; Bcl-2: B cell lymphoma protein-2; CCK-8: cell counting kit-8; SD: standard deviation; si: small interfering; NC: negative control; OD<sub>450</sub>: optical density at 450 nm; FITC: fluorescein isothiocyanate.

efficiency of si-*RAD51B* (Fig. 6d) and the overexpression efficiency of LV-*RAD51B-ASI* were verified (Fig. 6e). *RAD51B* expression levels increased following *RAD51B-ASI* overexpression (Fig. 6d), and the linear correlation between the two was verified (Fig. 6f). Immunohistochemical analyses confirmed that the expression levels of *RAD51B*, Ki67, and Bcl-2 proteins were significantly increased after *RAD51B-ASI* overexpression and were restored to their original levels in cells with simultaneous *RAD51B-ASI* overexpression and *RAD51B* knockdown (Fig. 6g). Taken together, these results supported our in vitro findings and suggested

that *RAD51B-ASI* may promote OC through *RAD51B* in vivo.

### 2.7 Correlation between high expression of *RAD51B-ASI* and poor prognosis

The correlation between *RAD51B-ASI* expression levels and the clinical prognostic parameters of 49 patients with OC was evaluated. The results revealed that higher *RAD51B-ASI* expression levels were positively correlated with poorer prognostic parameters, including FIGO stage and lymph node metastasis (Table 1). These results indicated that high

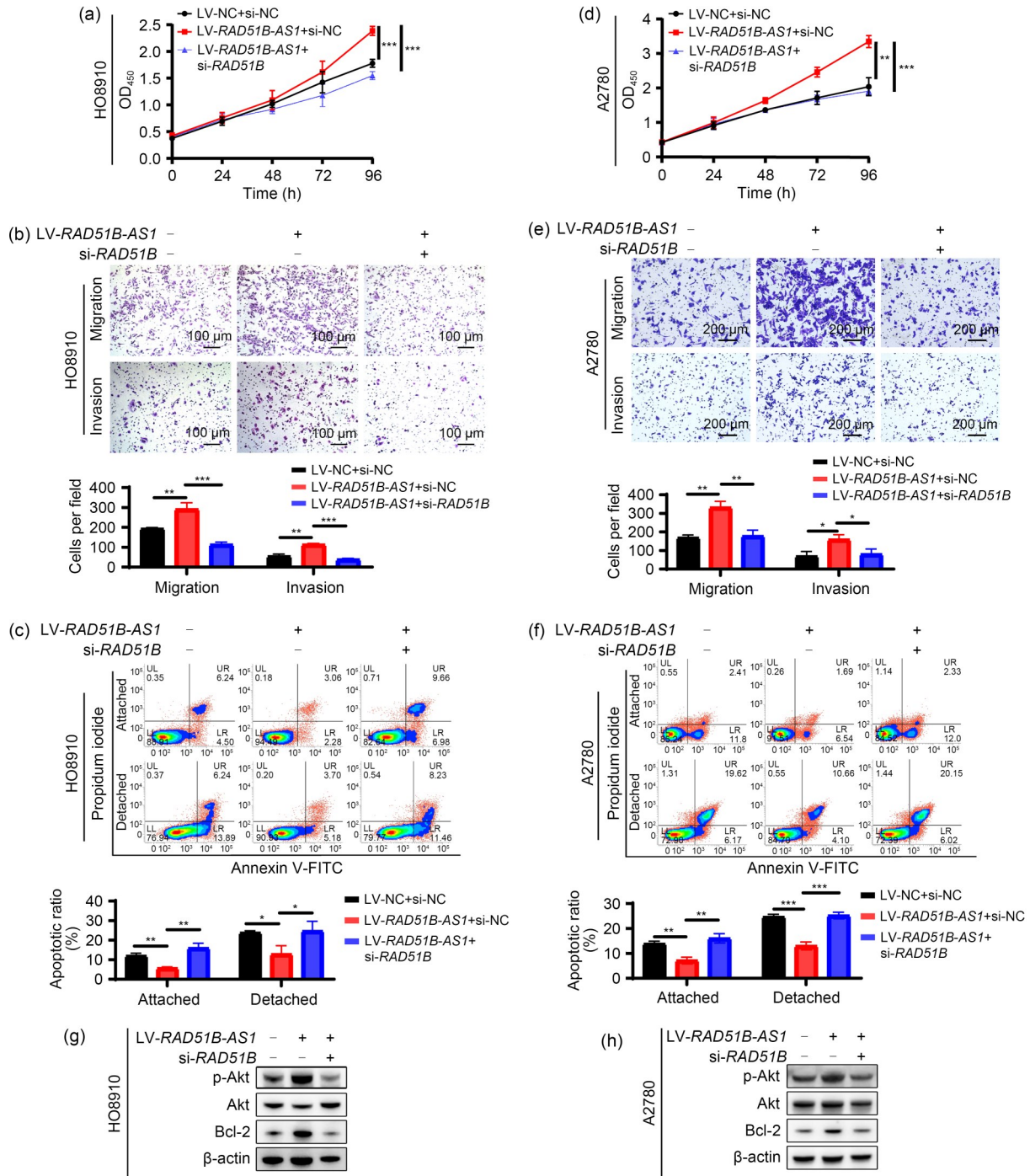


**Fig. 5** Effects of *RAD51B-AS1* on ovarian cancer (OC) progression and Akt/Bcl-2 pathway by regulating *RAD51B* expression. (a) CCK-8 assays were used to observe the growth of HO8910 cells. (b) Cell migration and invasion ability were observed using the transwell assay. (c) Apoptosis rates of adherent and suspended HO8910 cells were evaluated by flow cytometry. (d) Cell viability of A2780 cells was determined by CCK-8 assays. (e) Cellular migration and invasion were detected by transwell assay. (f) Cell apoptosis rates of adherent and suspended A2780 cells were evaluated by flow cytometry. (g, h) Total HO8910 cell lysates (g) and total A2780 cell lysates (h) were collected and immunoblotted with the indicated antibodies. Results are shown as mean±SD,  $n=3$ . \*  $P<0.05$ , \*\*  $P<0.01$ , \*\*\*  $P<0.001$ . Akt: protein kinase B; Bcl-2: B cell lymphoma protein-2; CCK-8: cell counting kit-8; SD: standard deviation; OD<sub>450</sub>: optical density at 450 nm; si: small interfering; NC: negative control; LV: lentivirus; FITC: fluorescein isothiocyanate; *RAD51B-AS1*: RAD51 homolog B-antisense 1.



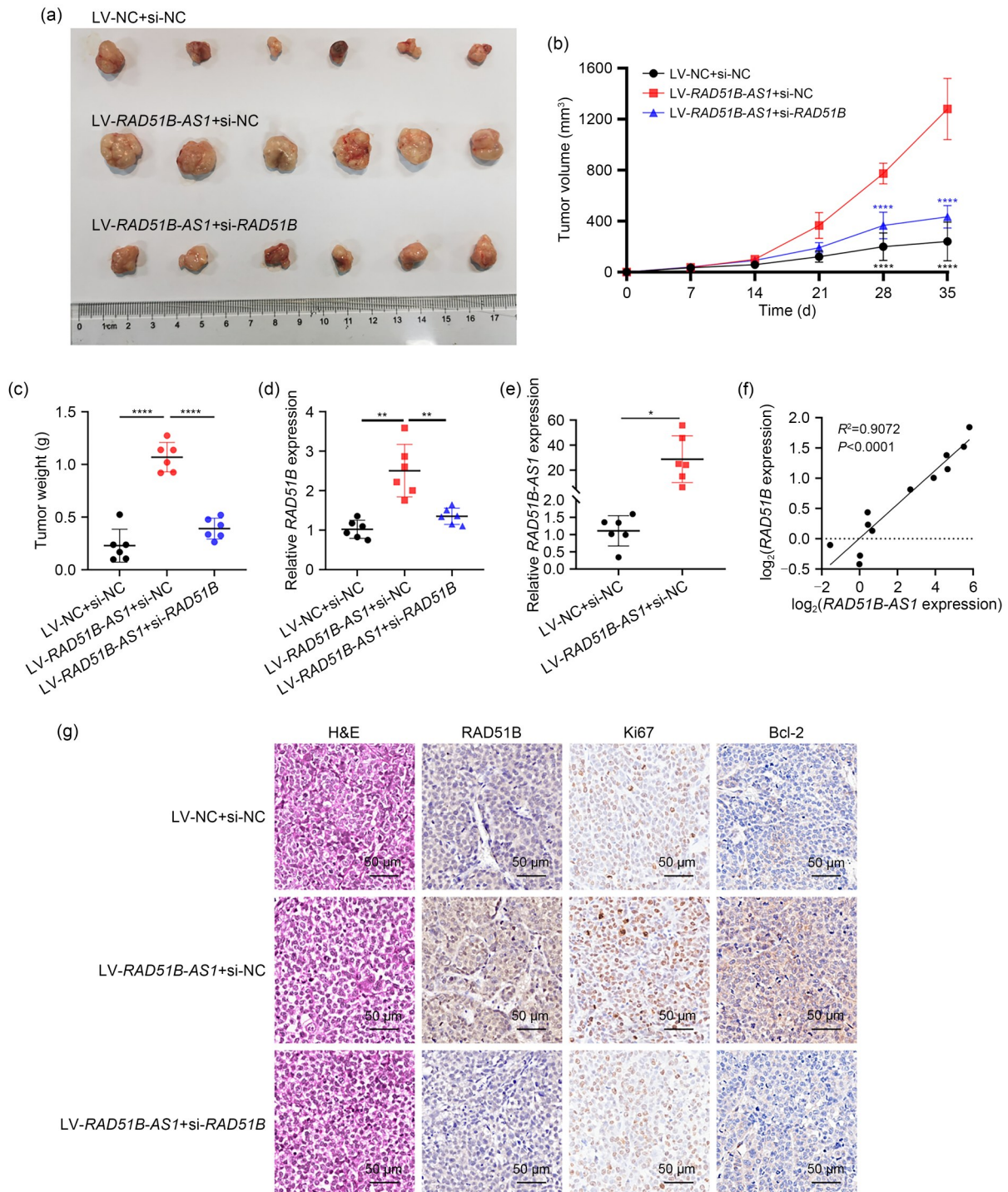


**Fig. 6** Effect of *RAD51B-AS1* on the progression of ovarian cancer by regulating *RAD51B* expression in vivo. (a) Final volume of subcutaneous neoplasms in nude mice. (b) The volume growth curve of subcutaneous tumors in nude mice. \*\*\*\*  $P<0.0001$ , vs. the LV-*RAD51B-AS1*+si-NC group. (c) Weight of the subcutaneous neoplasm in nude mice. (d) *RAD51B* expression in tumors was detected by RT-qPCR. (e) *RAD51B-AS1* expression in the tumor was detected by RT-qPCR. (f) Analyses of the linear relationship between lncRNA *RAD51B-AS1* and mRNA *RAD51B*. (g) IHC analyses of *RAD51B*, *Ki67*, and *Bcl-2*. Results are shown as mean±SD ( $n=6$ ). \*  $P<0.05$ , \*\*  $P<0.01$ , \*\*\*\*  $P<0.0001$ . *RAD51B-AS1*: *RAD51* homolog B-antisense 1; RT-qPCR: reverse transcription-quantitative polymerase chain reaction; lncRNA: long non-coding RNA; mRNA: messenger RNA; IHC: immunohistochemical; SD: standard deviation; *Bcl-2*: B cell lymphoma protein-2; si: small interfering; NC: negative control; LV: lentivirus; H&E: hematoxylin-eosin staining.

**Table 1 Association between *RAD51B-ASI* expression level and the clinicopathological parameters of patients**

Variable	Number	<i>RAD51B-ASI</i> expression		P value
		Low	High	
Age (years)				0.228
≤50	12	5	7	
>50	37	7	30	
FIGO stage				<b>0.012*</b>
I/II	10	6	4	
III/IV	39	6	33	
Lymph node metastasis				<b>0.044*</b>
Negative	23	9	14	
Positive	26	3	23	
Serum CA125 (U/mL)				0.183
≤500	23	8	15	
>500	26	4	22	

\* Bold values indicate  $P < 0.05$ .

*RAD51B-ASI* expression was a predictor of poor prognosis in patients with OC.

### 3 Discussion

To our knowledge, the present study is the first to uncover an uncharacterized lncRNA *RAD51B-ASI*, which was confirmed to be expressed at high levels in OC tissues and was markedly associated with unfavorable OC clinicopathological features, including FIGO stages III and IV and lymph node metastasis. In addition, *RAD51B-ASI* markedly promoted OC proliferation, migration, and anoikis resistance in vitro and in vivo. Previous studies have shown that anoikis is a key mechanism that prevents detached cells from surviving and attaching to a new matrix, thereby avoiding metastasis and the colonization of distant organs (Paoli et al., 2013; Jin et al., 2018; Nirmala and Lopus, 2020). Thus, we performed a series of experiments associated with anoikis and found that the overexpression of *RAD51B-ASI* significantly reduced the apoptotic rate of suspended cells and increased the anchor-independent growth of OC cells in the soft-agar assay. Furthermore, the intracellular RNA levels of lncRNA *RAD51B-ASI* in HO8910 cells were significantly increased after induction of the suspension for 24 and

48 h compared with adherent HO8910 cells. These results indicated that *RAD51B-ASI* contributed to anoikis resistance in OC. It has been reported that anoikis resistance is caused by the abnormal expression of certain genes or pathways, such as the Akt signaling pathway, of which the proteins of the Bcl-2 family are key players (Paoli et al., 2013; Zhou et al., 2014; Chen et al., 2018; Oudenaarden et al., 2018). Additionally, the activation of Akt, a central node of many signaling pathways, is critical for regulating a variety of cellular functions, including cell survival, proliferation, migration, metabolism, and angiogenesis, and is frequently deregulated in many types of human cancer (Ediriweera et al., 2019; Revathidevi and Munirajan, 2019; Tian et al., 2020). In this study, *RAD51B-ASI* overexpression could induce the phosphorylation of Akt and the activation of Bcl-2. Therefore, *RAD51B-ASI* may play an oncogenic role in OC.

The results of our study revealed that *RAD51B* expression was positively correlated with *RAD51B-ASI* expression and was significantly elevated in patients with OC. *RAD51B* downregulation suppresses OC malignancy, indicating its role as a tumor-promoting gene for OC. The transcript of *RAD51B-ASI*, functioning as an antisense lncRNA (aslncRNA), is complementary to the sense RNA strand of protein-coding gene *RAD51B*. AslncRNAs are widely expressed in a variety of tumors and cell lines (Katayama et al., 2005; Faghihi and Wahlestedt, 2009; Deng et al., 2019) and have the ability to perform multiple functions and act as positive or negative regulators of their homologous genes through cis or trans mechanisms (Zhang et al., 2017; Cui et al., 2021; Statello et al., 2021). However, the underlying mechanisms of action of antisense lncRNAs are complex. Depending on their localization, these RNAs can interact with DNAs, RNAs, and proteins to affect gene expression at the pre-transcriptional or post-transcriptional levels (D'Ydewalle et al., 2017; Su et al., 2017; Dang et al., 2021). This may involve mRNA splicing, stabilization of its complementary mRNA, mRNA localization and transport, and the initiation of sense-encoded proteins (Gibbons et al., 2018; Deng et al., 2019; Wu et al., 2019; Pan and Xie, 2020; Statello et al., 2021). However, the molecular mechanisms between aslncRNA and its host gene have not been fully explored. Further studies are required to understand in detail the underlying molecular mechanism through which *RAD51B-ASI* regulates *RAD51B*

and how both *RAD51B-ASI* and *RAD51B* activate the Akt/Bcl-2 signaling pathway.

*RAD51B* is a member of the human *RAD51* family, and *RAD51* protein levels are reportedly associated with genome instability, tumor recurrence, tumor progression, and increased resistance to radiotherapy and chemotherapy in various types of cancer (Woditschka et al., 2014; Huang et al., 2018; Zhang et al., 2019; Chiu et al., 2020; Chen et al., 2022; Wang et al., 2022). Interacting with breast cancer susceptibility genes 1/2 (*BRCA1/2*), *RAD51* was essential for DNA repair by homologous recombination, and *RAD51* inhibition sensitizes breast cancer stem cells to poly(ADP-ribose) polymerase (PARP) inhibitors (Liu et al., 2017; Cruz et al., 2018), which also provides a future direction for our further research. Further analyses are required to explore the function of *RAD51B-ASI* and *RAD51B* in the resistance to PARP inhibitors, especially in the subset of *BRCA1/2*-mutant OC patients.

These results may extend the current knowledge about potential biomarkers and their usefulness for predicting OS in patients with OC, and may guide therapeutic strategies for the disease. The results may also provide areas of study for determining the molecular mechanisms underlying the development of OC and provide new molecular markers and targets for the diagnosis and treatment of OC.

## 4 Conclusions

In summary, the current study demonstrated that the lncRNA *RAD51B-ASI* promoted the malignant biological behavior of OC, and the mechanism probably involved the activation of *RAD51B* and the Akt/Bcl-2 signaling pathway. These results may provide potentially effective therapeutic targets for certain types of OC.

## Materials and methods

Detailed methods are provided in the supplemental materials of this paper. In addition, the patient information is provided in Table S5. Primers' sequences are provided in Table S6. The sequences of probes for northern blotting are listed in Table S7. The sequences of siRNAs are listed in Table S8.

## Data availability statement

The data presented in this study are available from the corresponding author upon reasonable request.

## Acknowledgments

This research received no external funding. We thank all subjects who participated in this study and thank for the technical support by the core facilities, Zhejiang University, School of Medicine (Hangzhou, China).

## Author contributions

Weiguo LU, Junfen XU, Xiaodong CHENG, Xinyu WANG, and Xing XIE contributed to the study design. Xinyi WEI, Conghui WANG, Sangsang TANG, and Qian YANG performed the experimental research and data analysis. Xinyi WEI, Zhangjin SHEN, and Jiawei ZHU performed the establishment of animal models. Xinyi WEI, Weiguo LU, and Junfen XU wrote and edited the manuscript. Weiguo LU and Junfen XU revised the manuscript, and supervised and administrated the study. All authors have read and approved the final manuscript, and therefore, have full access to all the data in the study and take responsibility for the integrity and security of the data.

## Compliance with ethics guidelines

Junfen XU and Weiguo LU serve as Young Scientist Committee Member and Editorial Board Member, respectively, for *Journal of Zhejiang University-SCIENCE B (Biomedicine & Biotechnology)*, and were not involved in the editorial review or the decision to publish this article. Xinyi WEI, Conghui WANG, Sangsang TANG, Qian YANG, Zhangjin SHEN, Jiawei ZHU, Xiaodong CHENG, Xinyu WANG, Xing XIE, Junfen XU, and Weiguo LU declare that they have no conflict of interest.

The study was approved by the Ethics Committee of Women's Hospital, Zhejiang University School of Medicine, (approval number: IRB-20210147-R) for studies involving humans. All procedures followed were in accordance with the ethical standards of the responsible committee on human experimentation (institutional and national) and with the Helsinki Declaration of 1975, as revised in 2013. Informed consent was obtained from all patients for being included in the study.

The animal study protocol was approved by Institutional Animal Care and Use Committee (approval number: IACUC-20200506-07) for studies involving animals. All institutional and national guidelines for the care and use of laboratory animals were followed.

## Open Access

This article is distributed under the terms of the Creative Commons Attribution 4.0 International License (<http://creativecommons.org/licenses/by/4.0/>), which permits use, duplication, adaptation, distribution, and reproduction in any medium or format, as long as you give appropriate credit to the original author(s) and the source, provide a link to the Creative Commons license and indicate if changes were made.

## References

Bhan A, Soleimani M, Mandal SS, 2017. Long noncoding RNA and cancer: a new paradigm. *Cancer Res*, 77(15):

- 3965-3981.  
<https://doi.org/10.1158/0008-5472.Can-16-2634>
- Chen FF, Zhang L, Wu JQ, et al., 2018. HCRP-1 regulates EGFR-AKT-BIM-mediated anoikis resistance and serves as a prognostic marker in human colon cancer. *Cell Death Dis*, 9(12):1176.  
<https://doi.org/10.1038/s41419-018-1217-2>
- Chen LM, Yang PP, al Haq AT, et al., 2022. Oligo-Fucoidan supplementation enhances the effect of Olaparib on preventing metastasis and recurrence of triple-negative breast cancer in mice. *J Biomed Sci*, 29:70.  
<https://doi.org/10.1186/s12929-022-00855-6>
- Chiu WC, Fang PT, Lee YC, et al., 2020. DNA repair protein Rad51 induces tumor growth and metastasis in esophageal squamous cell carcinoma via a p38/Akt-dependent pathway. *Ann Surg Oncol*, 27(6):2090-2101.  
<https://doi.org/10.1245/s10434-019-08043-x>
- Cruz C, Castroviejo-Bermejo M, Gutiérrez-Enríquez S, et al., 2018. RAD51 foci as a functional biomarker of homologous recombination repair and PARP inhibitor resistance in germline BRCA-mutated breast cancer. *Ann Oncol*, 29(5):1203-1210.  
<https://doi.org/10.1093/annonc/mdy099>
- Cui XY, Zhan JK, Liu YS, 2021. Roles and functions of antisense lncRNA in vascular aging. *Ageing Res Rev*, 72:101480.  
<https://doi.org/10.1016/j.arr.2021.101480>
- Dang W, Cao PF, Yan QJ, et al., 2021. IGFBP7-AS1 is a p53-responsive long noncoding RNA downregulated by Epstein-Barr virus that contributes to viral tumorigenesis. *Cancer Lett*, 523:135-147.  
<https://doi.org/10.1016/j.canlet.2021.10.006>
- Deng SJ, Chen HY, Zeng Z, et al., 2019. Nutrient stress-dysregulated antisense lncRNA GLS-AS impairs GLS-mediated metabolism and represses pancreatic cancer progression. *Cancer Res*, 79(7):1398-1412.  
<https://doi.org/10.1158/0008-5472.Can-18-0419>
- D'Ydewalle C, Ramos DM, Pyles NJ, et al., 2017. The antisense transcript *SMN-AS1* regulates SMN expression and is a novel therapeutic target for spinal muscular atrophy. *Neuron*, 93(1):66-79.  
<https://doi.org/10.1016/j.neuron.2016.11.033>
- Ediriweera MK, Tennekoon KH, Samarakoon SR, 2019. Role of the PI3K/AKT/mTOR signaling pathway in ovarian cancer: biological and therapeutic significance. *Semin Cancer Biol*, 59:147-160.  
<https://doi.org/10.1016/j.semcancer.2019.05.012>
- Faghihi MA, Wahlestedt C, 2009. Regulatory roles of natural antisense transcripts. *Nat Rev Mol Cell Biol*, 10(9):637-643.  
<https://doi.org/10.1038/nrm2738>
- Gibbons HR, Shaginurova G, Kim LC, et al., 2018. Divergent lncRNA *GATA3-AS1* regulates *GATA3* transcription in T-helper 2 cells. *Front Immunol*, 9:2512.  
<https://doi.org/10.3389/fimmu.2018.02512>
- Huang J, Luo HL, Pan H, et al., 2018. Interaction between RAD51 and MCM complex is essential for RAD51 foci forming in colon cancer HCT116 cells. *Biochemistry (Mosc)*, 83(1):69-75.  
<https://doi.org/10.1134/s0006297918010091>
- Jin LT, Chun J, Pan CY, et al., 2018. The PLAG1-GDH1 axis promotes anoikis resistance and tumor metastasis through CamKK2-AMPK signaling in LKB1-deficient lung cancer. *Mol Cell*, 69(1):87-99.e7.  
<https://doi.org/10.1016/j.molcel.2017.11.025>
- Katayama S, Tomaru Y, Kasukawa T, et al., 2005. Antisense transcription in the mammalian transcriptome. *Science*, 309(5740):1564-1566.  
<https://doi.org/10.1126/science.1112009>
- Lheureux S, Gourley C, Vergote I, et al., 2019. Epithelial ovarian cancer. *Lancet*, 393(10177):1240-1253.  
[https://doi.org/10.1016/s0140-6736\(18\)32552-2](https://doi.org/10.1016/s0140-6736(18)32552-2)
- Liang HH, Yu T, Han Y, et al., 2018. LncRNA PTAR promotes EMT and invasion-metastasis in serous ovarian cancer by competitively binding miR-101-3p to regulate ZEB1 expression. *Mol Cancer*, 17:119.  
<https://doi.org/10.1186/s12943-018-0870-5>
- Liu YJ, Burness ML, Martin-Trevino R, et al., 2017. RAD51 mediates resistance of cancer stem cells to PARP inhibition in triple-negative breast cancer. *Clin Cancer Res*, 23(2):514-522.  
<https://doi.org/10.1158/1078-0432.Ccr-15-1348>
- Nirmala JG, Lopus M, 2020. Cell death mechanisms in eukaryotes. *Cell Biol Toxicol*, 36(2):145-164.  
<https://doi.org/10.1007/s10565-019-09496-2>
- Oudenaarden CRL, van de Ven RAH, Derksen PWB, 2018. Re-inforcing the cell death army in the fight against breast cancer. *J Cell Sci*, 131(16):jcs212563.  
<https://doi.org/10.1242/jcs.212563>
- Pan K, Xie Y, 2020. LncRNA FOXC2-AS1 enhances FOXC2 mRNA stability to promote colorectal cancer progression via activation of Ca<sup>2+</sup>-FAK signal pathway. *Cell Death Dis*, 11(6):434.  
<https://doi.org/10.1038/s41419-020-2633-7>
- Paoli P, Giannoni E, Chiarugi P, 2013. Anoikis molecular pathways and its role in cancer progression. *Biochim Biophys Acta*, 1833(12):3481-3498.  
<https://doi.org/10.1016/j.bbamcr.2013.06.026>
- Pei CL, Gong XJ, Zhang Y, 2020. LncRNA MALAT-1 promotes growth and metastasis of epithelial ovarian cancer via sponging microRNA-22. *Am J Transl Res*, 12(11):6977-6987.
- Revathidevi S, Munirajan AK, 2019. Akt in cancer: mediator and more. *Semin Cancer Biol*, 59:80-91.  
<https://doi.org/10.1016/j.semcancer.2019.06.002>
- Shen XM, Wang CH, Zhu HH, et al., 2021. Exosome-mediated transfer of CD44 from high-metastatic ovarian cancer cells promotes migration and invasion of low-metastatic ovarian cancer cells. *J Ovarian Res*, 14:38.  
<https://doi.org/10.1186/s13048-021-00776-2>
- Shen ZJ, Gu LK, Liu YW, et al., 2022. PLAA suppresses ovarian cancer metastasis via METTL3-mediated m<sup>6</sup>A modification of TRPC3 mRNA. *Oncogene*, 41(35):4145-4158.  
<https://doi.org/10.1038/s41388-022-02411-w>
- Statello L, Guo CJ, Chen LL, et al., 2021. Gene regulation by long non-coding RNAs and its biological functions. *Nat Rev Mol Cell Biol*, 22(2):96-118.

- <https://doi.org/10.1038/s41580-020-00315-9>
- Su WJ, Xu M, Chen XQ, et al., 2017. Long noncoding RNA ZEB1-AS1 epigenetically regulates the expressions of ZEB1 and downstream molecules in prostate cancer. *Mol Cancer*, 16:142.  
<https://doi.org/10.1186/s12943-017-0711-y>
- Sung H, Ferlay J, Siegel RL, et al., 2021. Global cancer statistics 2020: GLOBOCAN estimates of incidence and mortality worldwide for 36 cancers in 185 countries. *CA Cancer J Clin*, 71(3):209-249.  
<https://doi.org/10.3322/caac.21660>
- Tafer H, Hofacker IL, 2008. RNAplex: a fast tool for RNA-RNA interaction search. *Bioinformatics*, 24(22):2657-2663.  
<https://doi.org/10.1093/bioinformatics/btn193>
- Tian H, Lian R, Li Y, et al., 2020. AKT-induced lncRNA VAL promotes EMT-independent metastasis through diminishing Trim16-dependent vimentin degradation. *Nat Commun*, 11:5127.  
<https://doi.org/10.1038/s41467-020-18929-0>
- Torre LA, Trabert B, Desantis CE, et al., 2018. Ovarian cancer statistics, 2018. *CA Cancer J Clin*, 68(4):284-296.  
<https://doi.org/10.3322/caac.21456>
- US Preventive Services Task Force, 2018. Screening for Ovarian Cancer: US Preventive Services Task Force Recommendation Statement. *JAMA*, 319(6):588-594.  
<https://doi.org/10.1001/jama.2017.21926>
- Wang ZY, Jia RX, Wang LL, et al., 2022. The emerging roles of Rad51 in cancer and its potential as a therapeutic target. *Front Oncol*, 12:935593.  
<https://doi.org/10.3389/fonc.2022.935593>
- Woditschka S, Evans L, Duchnowska R, et al., 2014. DNA double-strand break repair genes and oxidative damage in brain metastasis of breast cancer. *J Natl Cancer Inst*, 106(7):dju145.  
<https://doi.org/10.1093/jnci/dju145>
- Wu DD, Chen X, Sun KX, et al., 2017. Role of the lncRNA ABHD11-AS<sub>1</sub> in the tumorigenesis and progression of epithelial ovarian cancer through targeted regulation of RhoC. *Mol Cancer*, 164:138.  
<https://doi.org/10.1186/s12943-017-0709-5>
- Wu WM, Gao H, Li XF, et al., 2019. LncRNA TPT1-AS1 promotes tumorigenesis and metastasis in epithelial ovarian cancer by inducing TPT1 expression. *Cancer Sci*, 110(5):1587-1598.  
<https://doi.org/10.1111/cas.14009>
- Wu YX, Gu WQ, Han X, et al., 2021. LncRNA PVT1 promotes the progression of ovarian cancer by activating TGF- $\beta$  pathway via miR-148a-3p/AGO1 axis. *J Cell Mol Med*, 25(17):8229-8243.  
<https://doi.org/10.1111/jcmm.16700>
- Xie WW, Sun HZ, Li XD, et al., 2021. Ovarian cancer: epigenetics, drug resistance, and progression. *Cancer Cell Int*, 21:434.  
<https://doi.org/10.1186/s12935-021-02136-y>
- Yang J, Peng SP, Zhang KQ, 2021. LncRNA RP11-499E18.1 inhibits proliferation, migration, and epithelial-mesenchymal transition process of ovarian cancer cells by dissociating PAK2-SOX2 interaction. *Front Cell Dev Biol*, 9:697831.  
<https://doi.org/10.3389/fcell.2021.697831>
- Zhang CL, Zhu KP, Ma XL, 2017. Antisense lncRNA FOXC2-AS1 promotes doxorubicin resistance in osteosarcoma by increasing the expression of FOXC2. *Cancer Lett*, 396:66-75.  
<https://doi.org/10.1016/j.canlet.2017.03.018>
- Zhang XM, Ma NY, Yao WQ, et al., 2019. RAD51 is a potential marker for prognosis and regulates cell proliferation in pancreatic cancer. *Cancer Cell Int*, 19:356.  
<https://doi.org/10.1186/s12935-019-1077-6>
- Zhao L, Jiang L, Zhang M, et al., 2021. NF- $\kappa$ B-activated SPRY4-IT1 promotes cancer cell metastasis by downregulating *TCEB1* mRNA via Staufen1-mediated mRNA decay. *Oncogene*, 40(30):4919-4929.  
<https://doi.org/10.1038/s41388-021-01900-8>
- Zhou ZZ, Deng H, Yan W, et al., 2014. AEG-1 promotes anoikis resistance and orientation chemotaxis in hepatocellular carcinoma cells. *PLoS ONE*, 9(6):e100372.  
<https://doi.org/10.1371/journal.pone.0100372>

### Supplementary information

Materials and methods; Tables S1–S8; Figs. S1–S3